Distributed model of hydrological and sediment transport processes in large river basins in Southeast Asia

S. Zuliziana[1,2], K. Tanuma[1], C. Yoshimura[1], O. C. Saavedra[1]

[1]Department of Civil Engineering, Tokyo Institute of Technology, 2-12-1-M1-4 Ookayama, Meguro-ku, Tokyo 152-8552, Japan

[2]Department of Civil Engineering, Faculty of Engineering, National Defense University of Malaysia, Sungai Besi Camp, 57000 Kuala Lumpur, Malaysia.

Corresponding author: S. Zuliziana (zulizianasuif@gmail.com)

Abstract

Soil erosion and sediment transport have been modeled at several spatial and temporal scales, yet few models have been reported for large river basins (e.g., drainage areas > 100,000 km^2). In this study, we propose a process-based distributed model for assessment of sediment transport at a large basin scale. A distributed hydrological model was coupled with a process-based distributed sediment transport model describing soil erosion and sedimentary processes at hillslope units and channels. The model was tested on two large river basins: the Chao Phraya River Basin (drainage area: 160,000 km^2) and the Mekong River Basin (795,000 km^2). The simulation over 10 years showed good agreement with the observed suspended sediment load in both basins. The average Nash–Sutcliffe efficiency (*NSE*) and average correlation coefficient (r) between the simulated and observed suspended sediment loads were 0.62 and 0.61, respectively, in the Chao Phraya River Basin except the lowland section. In the Mekong River Basin, the overall average *NSE* and r were 0.60 and 0.78, respectively. Sensitivity analysis indicated that suspended sediment load is sensitive to detachability by raindrop (k) in the Chao Phraya River Basin and to soil detachability over land (K_f) in the Mekong River Basin. Overall, the results suggest that the present model can be used to understand and simulate erosion and sediment transport in large river basins.

1 Introduction

Effective management of sediment in rivers is becoming increasingly important from an economic, environmental, and ecological perspective. A recent study of 145 major rivers with longer-term records of annual sediment loads showed that approximately 50% of them experienced a statistically significant upward or downward seasonal trend (Walling and Fang, 2003). The majority of them showed declining sediment loads because of dams and other river control structures trapping sediment. Moreover, human activities such as deforestation and water diversion might cause sedimentation or erosion in coastal regions. Such sediment-related problems could be more serious in the future because of further dam construction, climate variability, and deforestation (Walling, 2011; Zarfl et al., 2014). Currently, river basins in Southeast Asia have serious soil erosion potential and excessive sedimentation. They are also experiencing dramatic land surface changes, such as forest clearing, reservoir construction, and hydropower construction and water diversion (Tacio, 1993), because of rapid population and economic growth in the region (Walling, 2009).

A wide range of models exists for simulating erosion and sediment transport. These models differ in terms of complexity, processes considered, and the data required for model calibration and model use (Roberto et al., 2012). In general, there is no “best” model for all applications. The most appropriate model will depend on intended use, spatial scale, and characteristics of the catchment being considered. The Universal Soil Loss Equation (USLE) (Wischmeier and Smith, 1978) and its revised version (RUSLE) (Renard and Freimund, 1994) are widely used as tools for empirical assessment of soil erosion. Both USLE and RUSLE account for sediment eroded from the catchment in the long term (e.g., for 20 years). In these empirical equations, however, the deposition of sediment is not considered to occur in the modeled area.

A number of process-based soil erosion and sediment transport models have also been developed, but those applications are limited to individual storm events and small (max. 2.6 km^2) catchments (Du et al., 2009). The Soil and Water Assessment Tool (SWAT) was designed for application to large river basins and long-term simulations (Arnold et al., 1998) and has been implemented in river basins of over 4,000 km^2 (Santhi et al., 2001). It is a semi-distributed conceptual model, capable of daily simulation using hydrologic response units as the basic computational unit to group input information about combinations of land use and soil land management (Neitsch et al., 2002). However, semi-distributed models like SWAT do not generally incorporated with a fine resolution of spatial information, such as land use and soil information which are dominant factors affecting on soil erosion. Thus effective river basin management requires the development of process-based models to estimate the effects of the soil erosion rate, sediment transport, and deposition at specific locations and especially in large river basins.

Process-based models are based on the solutions of fundamental physical equations describing stream flow and sediment production in a river basin. They represent the physical processes observed in the real world, such as surface runoff, subsurface flow, groundwater flow, and evapotranspiration. Process-based models provide several major advantages over empirical and conceptual model, including capabilities estimating spatial and temporal distributions of net soil loss (or gain, in the case of deposition) for an entire hillslope or for each point on a hillslope. Further, process-based models can estimate sediment simulation on a daily, monthly, or an average annual basis. Since these models are process-based, they can also seasonally interpolated and extrapolated to some extent to a broad range of conditions, including some conditions that might be difficult to measure with field testing. Given the complexity of the relationships affecting sediment dynamics, it is important to develop a robust process-based model of sediment dynamics that can be used to predict the

consequences of natural systems as well as human-induced environmental changes and impacts, especially in large catchments.

This study aimed to develop a process-based distributed model that can simulate the sediment dynamic process at a large basin scale. The feasibility of the model was confirmed in large catchments (i.e., > 100,000 km^2) of Southeast Asia. The sediment model continuously simulates the sedimentary process, including erosion and sediment transport. Hydrologic data, soil type, land use, and topography were used as input data. Soil loss and its transport process were coupled with an existing distributed hydrological model to create a comprehensive sediment assessment tool for large catchments in Southeast Asia. The sediment model separately simulated deposition and detachment in rivers, which have not been considered in most existing models. This paper also describes applications of the sediment model in two large river basins in Southeast Asia: the Chao Phraya and Mekong River basins. The two basins are characterized by different soil properties and hydrogeology.

2 Model structure

The important processes of sediment dynamics (soil erosion, sediment transport, and deposition) were modeled and integrated with a process-based distributed hydrological model (DHM) (Fig. 1). In the sediment model, sediment dynamics on hillslopes and rivers were separately modeled and systematically linked each other. The sediment model was developed using FORTRAN to create a compatible link to the adopted distributed hydrological model. The runoff and river routing were incorporated within the sediment model. Hydrological and sediment-related processes were calculated on a daily time-step. The overall model was designed to target suspended sediment load (SSL), because suspended sediment (SS) is dominant portion of the transported sediment in many of the world's rivers (Ongley, 1996),

and it is frequently assumed that the suspended load makes up about 90% of the total load in the world (Milliman and Meade, 1983).

2.1 Hydrological model

The distributed hydrological model used in this study is a geomorphology-based hydrological model (GBHM) developed by Yang et al. (2001). It solves the continuity, momentum, and energy equations using two modules: hillslope module and river routing module.

In the GBHM, the target watershed is divided into grids, and a digital elevation model (DEM) is used to determine the flow direction and accumulation pattern that creates the river network. Each subbasin is divided into a number of flow intervals. In the subbasins, flow intervals are defined as a function of distance from the subbasin's outlet. Lateral flow to the main stream is estimated by accumulating runoff at each grid in one hillslope unit. This means that all hillslopes of a flow interval drain into the main stream in this model. The flow interval–hillslope system enabled the GBHM to realize a fast flow computation even in a large basin. The hillslope unit is viewed as a rectangular inclined plane with a defined length and unit width. The inclination angle givens by the corresponding surface slope.

In the hillslope model, each soil is divided into four layers: canopy, soil surface, unsaturated zone, and groundwater. Vegetation covered the surface soil and prevented direct rainfall onto the land. The deficit of canopy interception is calculated by vegetation coverage and leaf area index. The evapotranspiration module simulated the water volume that evaporated from the surface soil and transpirated from the canopy, where pan observation could also be used. In the module, Priestley–Taylor's method was applied for the canopy water storage, root zone, surface storage, and soil surface. In order to describe the unsaturated zone water flow, a vertical one-dimensional Richards equation is used with soil infiltration rate and soil moisture contents in the root zone. Saturated water flow and exchange with the

river is described using basic mass balance equations and Darcy's Law. The simulation module of surface water flow estimated the infiltration excess and saturation excess discharging into the river system as lateral flow.

In the river routing system, the Pfafstetter numbering system is applied to track water flow efficiently from upper to downstream. The water routing on the river network is determined along the river stream using one-dimensional kinematic wave equations. Further details are described by Yang et al. (2001).

2.2 Sediment model

2.2.1 Soil detachment

Soil detachment by raindrop impacts was estimated by Eq. (1) (Torri et al., 1987).

$$D_{\mathrm{R}} = \left(1 - C_{\mathrm{g}}\right) k E e^{-zh} \quad (1)$$

where D_{R} is soil detachment rate by raindrop impact (g m^{-2} hr^{-1}) estimated for each time step, k is an index of the detachability of the soil (g J^{-1}), E is the total kinetic energy of the rainfall (J m^{-2} hr^{-1}), e^{-zh} is the correction factor for water ponding where z depends on soil texture (0.9–3.1), and h is the depth of the surface water layer (mm). C_{g} is the proportion of soil surface in each grid. Raindrop impacts were categorized into direct rainfall and leaf drip, allowing the total kinetic energy (E) of raindrop to be described by Eq. (2).

$$E = (1 - C_{\mathrm{C}}) E_{\mathrm{D}} H_{\mathrm{DT}} + C_{\mathrm{C}}\, E_{\mathrm{L}} H_{\mathrm{LD}} \quad (2)$$

where C_{C} is canopy cover in the model (i.e., in each grid) and was estimated from land use data on a scale of 0.0 to 1.0 (0 for bare land and 1.0 for highly dense forest area). E_{D} is the kinetic energy of direct throughfall drops (J m^{-2} mm^{-1}), and H_{DT} is depth of direct throughfall drops, for which rain intensity (mm hr^{-1}) was used in the model. E_{L} is the kinetic energy of

leaf drip (J m^{-2} mm^{-1}), and H_{LD} is the depth of leaf drip (net rain (mm hr^{-1})), which was estimated by deducting the interception loss of water from the depth of rain intensity (H_{DT}).

The kinetic energy for direct rainfall E_D can be described by Eq. (3) (Brandt, 1989) where I is rain intensity (mm hr^{-1}).

$$E_D = 8.95 + 8.44 \log(I) \quad (3)$$

E_L is the kinetic energy due to leaf drip, also as proposed by Brandt (1990) and shown in Eq. (4). PH is the effective height of the plant canopy in meters. This study assumed that PH is 1 meter following Kabir et al. (2011).

$$E_L = (15.8(PH)^{0.5}) - 5.87 \quad (4)$$

For soil detachment due to overland flow, we used equations derived by Habib-ur-Rehman and Akhtar (2004) and shown as Eq. (5) and (6). These were used to compute soil detachment based on comparison of critical shear stress and hydraulic shear stress.

$$D_F = K_f\left(\frac{\tau}{\tau_c} - 1\right) \quad \text{for} \quad \tau > \tau_c \quad (5)$$

$$D_F = 0 \quad \text{for} \quad \tau < \tau_c \quad (6)$$

where D_F is an overland flow detachment (kg m^{-2} s^{-1}), K_f is an overland flow detachability coefficient (kg m^{-2} s^{-1}), τ_c is critical shear stress for initiation of soil particle motion as obtained from the Shield's curve (N m^{-2}) and τ is hydraulic shear stress (N m^{-2}) as given in Eq. (7).

$$\tau = \gamma h S \quad (7)$$

where γ is a specific weight of water (N m^{-3}) and h is depth of overland flow (m). In this study, the depth of overland flow is assumed to be the corresponding surface water depth. S is

the slope of the ground surface. In Eq. (5), K_f is subjected to calibration and the critical shear stress values are obtained by the following equation.

$$\tau_C = N_{sheilds}(\gamma_s - \gamma)D_s \quad (8)$$

where $N_{sheilds}$ is the value of the dimensionless shield parameter obtained from the Shield's curve, γ_s is the specific weight of sediment particles (N m^{-3}), γ is a specific weight of water (N m^{-3}) and D_s is sediment particle size (μm).

2.2.2 Transport and deposition of sediment

Soil detachments by flow and sediment deposition in rivers are generally considered to occur simultaneously. Flow detachment or deposition can be expressed by Eq. (9), as described by Morgan et al. (1998).

$$DF_{river} = \beta_s w v_s (TC - C_s) \quad (9)$$

where DF_{river} is the flow detachment or deposition of sediment (m^3 s^{-1} m^{-1}) for sediment concentration C_s (m^3 m^{-3}), TC is the transport capacity (m^3 m^{-3}), w is the width of the river flow (m) in each subbasin as estimated from the input parameter of the hydrological model and v_s is particle settling velocity (m s^{-1}) calculated with Stokes's Law. β_s is a correction factor used to calculate cohesive soil erosion as shown in Eq. (10) (Kabir et al., 2011).

$$\beta_s = 0.79e^{-0.85J} \quad (10)$$

where J is the soil cohesion (kPa). Several methods have been developed to estimate TC. This study adopted Eq. (11), proposed by Govers (1990), because of its simple structure and available input parameter database. Eq. (11) was only used to estimate SSL, not including bed loads.

$$TC = c(\omega - \omega_{cr})^{\eta} \quad (11)$$

where ω is the unit stream power (cm s^{-1}), $\omega = 10Vs$, V is mean flow velocity (cm s^{-1}), s is the slope in percentage, and ω_{cr} is the critical value of unit stream power (0.40 cm s^{-1}). In this study, 2.65 g cm^{-3} of soil density was used for the conversion unit in both case studies. c and η are coefficients that depend on the median particle size of the soil (d_{50} in μm).

$$c = [(d_{50} + 5)/0.32]^{-0.6} \quad (12)$$

$$\eta = [(d_{50} + 5)/300]^{0.25} \quad (13)$$

The movement of sediment in each grid cell was determined by associating the movement with water discharge, based on the principle of conservation of mass and momentum similar to the flow simulation in the distributed hydrological model. The one-dimensional kinematic wave and finite difference approximation were applied to simulate sediment transport both over land and in the river. On the land grids, the movement of soil and water flow was accumulated at each flow interval with a weighting system that was based on the distance from the main stream. Then, the accumulated flow was streamed into the river as lateral flow. The water discharge (Q) was determined by the one kinematic wave approximation in the river node. The kinematic wave equation shown in Eq. (14) was also applied to the river routing model to calculate the movement of suspended sediment concentration (Cs) by using the given Q. Using Eq. (9) and (15), Eq. (14) was converted to Eq. (16).

$$\frac{\partial Q_s}{\partial x} + \frac{}{\partial t} = qs(iflow) + DF_{river} \quad (14)$$

$$Q_s = QC_s; Q = AV;\ Q_s = AV \quad (15)$$

$$\frac{\partial (QC_s)}{\partial x} + \frac{\partial (\frac{QC_s}{V})}{\partial t} = qs(iflow) + \beta_s w\, v_s\, (TC - C_S) \quad (16)$$

where Q is river discharge from the hydrological model (m^3 s^{-1}), A is the cross-section area (m^2) of water and sediment flow, V is stream velocity (m s^{-1}), qs is accumulated sediment

yield (m^3 s^{-1} m^{-1}) in flow-interval and *if* is the number of flow intervals in each subbasin. An accumulated sediment yield was considered as the lateral sediment flow and was added at the inlet of the control volume (i.e., the river routing part). In the river routing, the unit of sediment mass (g) was changed to volume (m^3) by dividing with the specific weight of sediment (2.67 g cm^{-3}).

2.3 Dam model

The inflow to a dam, Q_{in}, was calculated at its upstream flow interval right before the dam location on a river network by GBHM. The balance of dam inflow and outflow is described by change of reservoir storage in time using Eq. (17) (Ponce, 1989).

$$I - O = \frac{d\forall}{dt} \tag{17}$$

where I is inflow, O is an outflow, $d\forall$ is change in storage volume within a time interval (dt). Then, the reservoir storage at the current time step $\forall_2$ was obtained per Valeriano et al. (2010),

$$\forall_2 = \forall_1 + \left[\left(\frac{Q_{in}^1 + Q_{in}^2}{2}\right) - Q_{out}^2\right]\Delta t \tag{18}$$

where the subscript 1 refers to the last time step, and the subscript 2 refers to the current time step. Q_{out}^2 is discharge from the dam and is assumed to be constant between time steps 1 and 2. Both inflows Q_{in}^1 and Q_{in}^2 are discharge flow into the dam and are provided by the simulation using GBHM. The value for the last time step volume $\forall_1$ needs to be set as the initial volume condition to read the h-∀ curve data. Then, using the h-∀ curve, the water level can be calculated. In normal conditions, the release can be calculated using a dam operational rule. Once the release is defined, the flow can be routed downstream by GBHM.

In the following case studies, the dam operation rule was applied, and release was assumed to be equal to observed release from the Bhumibol and Sirikit dams in the Chao Phraya River Basin. In contrast, in the Mekong River Basin, the mean annual discharge from the Lancang

subbasin (2,332.29 $m^3 s^{-1}$) (Kummu et al., 2010) was used as dam release at Manwan Dam, assuming that hydropower station stabilizes its downstream river discharge. In the Chao Phraya River Basin, the reservoir sedimentation was estimated by Brune's curve (Brune, 1953). No estimation of reservoir sedimentation in the Mekong River Basin was made, due to limited availability of dam observation data.

3 Model application

3.1 Chao Phraya River Basin

The Chao Phraya River Basin covers about one third of Thailand, which is approximately 160,000 km^2 from head to mouth. In this study, the target basin covered from sources to the Chao Phraya Dam (C13) (the gray area in Fig. 2), which has a catchment area of 117,375 km^2. The basin is traditionally the center of Thailand's rice production, because the monsoon weather typically brings rice rainfall from May to October. Land cover in the Chao Phraya River Basin consists of forest (30.2%, including evergreen, deciduous and mangrove forests), croplands (56.4%), paddy fields (7.1%), bodies of water (0.6%), and areas for which no data is available (5.7%) (UNEP, 1997). The soil in the Chao Phraya River Basin is predominantly sand clay loam and contains 38.2% sand, 25.2% silt, and 36.7% clay on average (Kyuma, 1976). The Chao Phraya River has four major tributaries: the Ping River (36,018 km^2), the Wang River (11,708 km^2), the Yom River (24,720 km^2), and the Nan River (34,557 km^2). They converge at Nakhon Sawan. In the northern mountainous region, there are valleys covered by forest and bare soil. These valleys stretch south to north, which is the area of the headwaters of the Chao Phraya River Basin.

The climate in Thailand is strongly affected by the Southeast Asian monsoon and characterized by distinct rainy and dry seasons. Basically, the rainy season starts at the middle

or end of May and lasts until the middle of October. Annual precipitation in the Chao Phraya River Basin varies between 1,000 and 1,500 mm (Thai Meteorological Department, 2012).

3.1.1 Model set-up and calibration

Geographical information for the Chao Phraya River Basin (e.g., topography, soil type, and land use) was collected for the development of a hydrological model. A DEM was obtained from the Shuttle Radar Topography Mission (URL: http://dds.cr.usgs.gov/srtm/version2_1/SRTM3/). The model has 90 m spatial resolution. In the study area, the resolution was aggregated to 1 km for simulation. Soil type classification relied on the Digital Soil Map of the World (version 3.6) from the Food and Agriculture Organization of the United Nations (FAO/UN). The dominant soil is clay and sand in the upper region and sandy silt in the lower region. Land use data (2001) were obtained from the Land Development Department of Thailand (http://www.ldd.go.th/). The land use categories are paddy field, farm land, forest, grassland, bare land, urban area, and water body. Daily precipitation data were collected from two kinds of rain gauge network systems. The first is open-source rain gauge network data provided by the Hydrology and Water Management Center for the upper northern region of the Royal Irrigation Department (RID). The other is managed by the Thai Meteorological Department (TMD). Both data sources have daily temporal resolution. Daily dam operational data such as water level, storage, inflow, and outflow (release) for the Sirikit Dam and Bhumibol Dam were gathered from RID and the Electricity Generating Authority of Thailand (E-GAT).

River discharge and SSL were calibrated and validated in combination with dam operation for the period from 2001 to 2010 at four stream gauges in the upper region (P73-Ping River, W3A-Wang River, Y37-Yom River, and N13A-Nan River) and one stream gauge in the outlet (C2-Chao Phraya River) (Fig. 2). Taking into account the availability of data, the monthly river discharge and SSL data for 2001 were used for the calibration model at all five stream

gauges, whereas the observation data from 2002–2010 were used for validation. For the parameter calibration, a semi-automatic calibration method was used. It was the Shuffled Complex Evolution (SCE) algorithm (Duan et al., 1992). It was implemented in 2001 to identify suitable parameters. The dominant factors affecting the hydrological process and soil erosion, such as land use and soil characteristics, were considered for parameter calibration, as listed in Table 1. As for parameters related to sediment transport and soil erosion, the FAO global soil dataset was used to consider spatial distribution of soil properties. The parameters of sediment detachability from rain drop (k) and from sheet flow (K_f) in the basin were calibrated respectively based on the observed SSL at Khong Chiam. Soil cohesion (J) was determined in each subbasin. In the sediment model, the sediment particle size (d_{50}) was assumed to be 50 μm based on the suspended sediment distribution in a river near Chiang Mai (unpublished data). To demonstrate the applicability of the proposed model, the model was calibrated and validated with two efficiency criteria: the Nash–Sutcliffe efficiency coefficient (*NSE*) and correlation coefficients (r) for 2001–2010. Lastly, the eleven soil types in the Chao Phraya Basin were reclassified into three types: clay, sand, and silt.

3.1.2 Results and discussion of model performance

The monthly calibration for the hydrological and sediment process was implemented with SCE in Chao Phraya in 2001 (Table 1). The parameters for sediment (k, J) were calibrated to be larger than the reported values (Morgan et al., 1998), but they are within the reasonable range for the Chao Phraya River Basin (Bhattarai and Dutta, 2005).

Model evaluation revealed that the river discharge simulation performed satisfactorily, as shown by *NSE* and r in Table 2 (refer to Appendix A for hydrographs). The values of *NSE* and r at P73 were closer to 1 than in other drainage basins and were the lowest at C2 among the gauges. The reason for the lowest *NSE* occurring at the downstream gauge is related to the flooding situation in the Chao Phraya River Basin. Normally, the river discharge overflows

every year during rainy season in the lower region because the discharge capacity around C2 is low. Therefore, the overestimated discharge is likely to overflow to land in real situations. Moreover, the average slope is 1.3% in the lower basin, whereas it is 3.1% in the upper mountainous region where surface water can inflow smoothly to the river channel. Thus, the condition lengthens retardation time and river discharge gets stuck in the lower regions. In addition, water withdrawal for irrigation canals, which was not modeled in this study, also has an effect on the lowest hydrological situation in the lower region.

Regarding SSL, *NSE* for all stream gauges was larger than 0.5 except at C2 (Table 2). The simulation results captured the high peak of SSL during rainy season, as shown in Fig. 3. Overall, the performance of the model in the Chao Phraya River Basin indicated sufficient accuracy for long-term simulation (Table 2). The results from C2, located at the lowest reach, were not as good as in other stream gauges. At C2, the results indicate underestimation, even though the total simulated river discharge at the lower reach was overestimated and supposedly resulted in higher simulated SSL in the lower reach than in the upper reach. However, it appears the simulation error may have been larger at the lower reach because of accumulating uncertainty. The average total annual SSL was estimated to be 1.28×10^6 t yr^{-1} showing a ten-year increase from 5.72×10^6 to 8.10×10^6 t yr^{-1}. This estimate was slightly lower than the reported estimate of the average total annual SSL in the Chao Phraya River Basin (11×10^6 t yr^{-1}), as reported by FAO/AGL (2005). The different locations of the control points could be a reason for these different estimates of SSL.

It is inferred that the process of soil loss was strongly influenced by rainfall intensity. This was clearly shown by the simulated SSL at the Nan River (Fig. 3), where rainfall is higher (1,341.8 mm) than at other tributaries. In contrast, the simulated SSL was lowest at the Wang River due to that area having the lowest annual average rainfall (1,181.3 mm). Walling (2009) reported that the annual SSL in Chao Phraya declined from around 28×10^6 t yr^{-1} in the

1960s and early 1970s to around 6×10^6 t yr^{-1} in the 1990s. In this study, the average annual SSL was estimated to be 1.28×10^6 t yr^{-1} over 10 years based on simulation in the 2000s. In fact, the observed SSL shows a decreasing trend with a decline in annual runoff, primarily reflecting the trapping of sediment by a large number of small dams and irrigation structures and also by the larger Bhumibol and Sirikit dams (Walling, 2009). But for the 10 years targeted in this study, the observed SSL at C2 shows no decreasing trend. Nevertheless, climate change, population growth, land clearance, land use change, reservoir construction, and other infrastructure development can be expected to cause some changes in the SSL over the longer-time scale of 50 years in large river basins like the Mekong River Basin (Walling, 2011).

The simulated SSC also shows good correlations with observed data at all upper stream gauges, indicated by r larger than 0.5 except at the watershed outlet, C2 (Table 2). Possible errors in simulated SSC at the outlet could be related to river discharge simulation. The overall average relative mean square error (RMSE) between simulated and observed SSC ranged from 0.07 to 0.09 kg m^{-3} in the upper basins (P73, W3A, Y37, and N13A) and 0.09 kg m^{-3} in the outlet, C2. Basically, we confirmed two peaks every year in both observed and simulated SSC in four stream gauges: P73, W3A, Y37, and N13A (Fig. 4). The first peak occurred in May, which is the beginning of the rainy season. Beginning in June, the concentration fell while river discharge increased from the upper stream, due to the starting rainy season. The second peak occurred in the main monsoon periods (August, September, and October), which have heavy rainfall that increases the volume of river discharge.

3.1.3. Sensitivity of SSL to sediment-related parameters

The sensitivity of modeled SSL was also investigated for the reasonable ranges of the input parameters. The target parameters for this sensitivity analysis were soil detachability from

rain drop (k), soil detachability from sheet flow (K_f), and soil cohesion (J). The target period for this analysis was one year 2005 at P73.

First, results were obtained by changing the detachability of soil (k) from 7.0 (for clay and silt) and 9.1 (for sand) (g J^{-1}) by +50, -50, and -75% from those calibrated values. The theoretical range of this soil detachability index is 0.01 to 10 g J^{-1}, where the minimum is for clay, and the maximum is for sand (Gumiere et al., 2009; Morgan et al., 1998; Morgan, 2001). The peak of SSL increased as the detachability increased (Fig. 5a). The calibrated parameter k for dominant clay soil (7.0 g J^{-1}) was larger than one for the dominant sandy soil in the Chao Phraya River Basin (3.5 g J^{-1}, Bhattarai and Dutta, 2005) and one for a wide range of soil texture that are commonly used for agriculture in Europe (2.0 g J^{-1}, Morgan et al., 1998). Basically, the soil detachability is associated with soil texture, showing a higher detachability with a lower clay content. Thus, soils having a high clay content are difficult to detach by raindrops (Sharma et al., 1994). In the Chao Phraya River Basin, detachability (k) was relatively high, indicating high soil detachment and resulting in high SSL transport into the river. The presented results reveal the importance of raindrop detachment for different type of soils, especially for clay soil in the Chao Phraya River Basin.

Second, we focused on K_f, which indicates soil detachability from sheet flow (Eq. 5). The initial values of K_f (0.6 (clay), 1.0 (silt), and 1.1 mg m^{-2} s^{-1} (sand)) were shifted by the factors 100, 10, 0.1, and 0.01 (Fig. 5b) in each type of soil; clay, silt and sand. The results show that the simulated suspended sediment peaks (August to October) increased slightly as K_f increased, although the changes were small and invisible in Fig. 5b. Thus, SSL is less sensitive to K_f than k, which is possibly because the precipitation is the main agent for sediment yield.

Third, soil cohesion (J) was shifted by +25% -25% and -50% from the calibrated value (3.0 kPa). Each model output was confirmed to understand the degree of net soil detachment

in streams influenced by transport capacity. The peak of SSL in September increased as *J* increased (Fig. 5c). In this case, the lateral inflow of sediment was the same as the initial results with 3.0 kPa. Eq. (10) and Eq. (11) infer that soil erosion increases SSC as higher *J* under saturated SSC condition (i.e., $T_c > C_s$) contributes to less deposition. Generally, *J* needs to be adjusted considerably to properly predict the measured net soil loss, since *J* is related to erodibility and limits detachment within river sediment. The simulated SSL from the LISEM model consistently increased with measured SSL and with increasing *J* (range from 2 to 7 kPa) (Nearing et al., 2005).

Sensitivity analysis was conducted for three parameters to evaluate the reliability of the model for simulating sediment dynamics. Overall, the two input parameters (*k and J*) that describe soil erodibility showed the significant influence on SSL in the Chao Phraya River Basin. The range of input parameters used in this model could be a useful reference for sediment-related research in the Chao Phraya River Basin.

3.2 Mekong River Basin

The second study area was the Mekong River Basin, covering an area of approximately 795,000 km^2. The Mekong is the largest trans-boundary river in Asia (Fig. 6). It originates in Tibet and flows down to Southern Vietnam, a distance of more than 4,600 km. The minimum and maximum annual rainfalls in the basin are 1,000 mm $year^{-1}$ (northeast of Thailand) and 4,000 mm $year^{-1}$ (west of Vietnam), respectively (Kite, 2001). The wet season lasts from May to October. During the wet season, average rainfall reaches around 80–90% of the annual total. The dry season starts in November and lasts until April. In this study, the area of the modeled basin is 786,335 km^2, not including the delta in southern Vietnam.

In this basin, acrisols were found to be the dominant soil type. These are tropical soils that have a high clay accumulation in a horizon and are extremely weathered and leached. Their characteristics include low fertility and ease of erosion if they are used for arable cultivation.

The average textures of soils in the Mekong River Basin are 27.1% sand, 30.4% silt, and 42.5% clay (Kyuma, 1976). The forest coverage in the Mekong River Basin is 30.5%. The agricultural land coverage is 40.7%. The rest of the areas are shrubland (17.2%), urban (2.1%), and water bodies (8.7%) (MRC, 2000). This study examined the model outputs (river discharge, SSL, and SSC) at three hydrologic stations; 1-Chiang Sean, 2-Khong Chiam, and 3-Phnom Penh (Fig. 6).

3.2.1 Model set-up and calibration

The input data for the model include weather data, topography data, soil properties and land cover. In this study, the GTOPO30 global DEM data with a horizontal grid spacing of ~20 km^2 (grid area: 2 × 2 min) resolution was used to delineate the Mekong River Basin. The land cover and soil type for the basin were obtained from Global Land Cover 2000 (http://edc2.usgs.gov/glcc/eadoc2_0.php) and the FAO soil map of the world (FAO, 2003), respectively. The elevation data was first converted to 3.6 km × 3.6 km resolution, and land cover and soil data were aggregated by reclassifying the land use data for nine classes and the soil data for eight classes. Daily precipitation and air temperature data from 65 station weather stations were obtained from the Mekong River Commission (MRC).

Annual records of river discharge and SSC in the study were extracted from the historical record published by the MRC (Mekong River Commission, 2005). The historical record tabulated measurements of river discharge, SSC, water quality, and other physical characteristics at gauging stations located along the Mekong River Basin and those of the river's tributaries. In this study, river discharge and SSC records from the three targeted stations were identified and used to calibrate and validate SSL simulation. The stations were selected based on their relative locations and the completeness of river discharge and sediment records at the station. Unlike river discharge, which was measured daily, SSC was monitored monthly. SSC samples were collected near the surface of the river (0.3 m depth) in

the middle of the main stream (MRC, 2000). In this study, monthly observed SSL was computed from the monthly measured SSC and the corresponding measured daily river discharge.

The river discharge and SSL were simulated by considering an existing dam in the Chinese section of the main stream (Manwan Dam). The model simulated river discharge, SSL, and SSC for 10 years from 1991 to 2000, and three stream gauges along the main stream were adopted for calibration and validation (Fig. 6). The daily river discharge and sediment data for the period from 1991–1995 were used for calibration, whereas the data from 1996–2000 were used for validation. For the sediment particle size (d_{50}), 50 μm were adopted in this study area because all the sediment is commonly < 62 μm in diameter (i.e., silt and clay), and sediments less than 2 μm make up 45% of the section near Vientiane (Ahlgren and Hessel, 1996). The five parameters shown in Table 1 were initialized with empirical values and then calibrated according to the observed river discharge and SSL at the three gauges. All the parameters were calibrated by SCE (Duan et al., 1992). Observation at Chiang Sean was used for calibration of parameters that reflect only the upper basin, whereas observation at Khong Chiam was used for calibration for the middle basin and observation at Phnom Penh was used for the lower basin. The fit between simulated and observed results (river discharge and SSL) was evaluated using the *NSE* (Nash and Sutcliffe, 1970) and correlation coefficients (*r*) at monthly intervals from 1991–2000.

3.2.2. Results and discussion of model performance

The river discharge of the Mekong was well simulated at all three stations (Table 3) (refer to Appendix B for hydrographs). The *NSE* values for river discharge at Chiang Sean, Khong Chiam and Phnom Penh were larger than 0.7 for calibration and validation from 1991–2000. The average correlation *r* between observation and simulation discharge was equally high (*r* >

0.8). These indicators imply the GBHM satisfactorily describes the seasonal cycle and spatial distribution of the hydrology processes in the Mekong River Basin, although the simulated discharge showed slightly higher peaks.

For the sediment model, we calibrated the same parameters as in the Chao Phraya River basin. In the Mekong River, wider ranges were determined for k and K_f, whereas the range of J narrowed slightly due to different physical characteristic such as topography (e.g., rill, interill, and gully) and structure of soil (e.g., erodibility and type of soil content). For example, the range of k for the Mekong (7.0–100.0 kg J^{-1}) is wider than that for the Chao Phraya (7.0–9.1 kg J^{-1}) (Table 1). This is probably because of the soil structure and content. The Chao Phraya River Basin is mostly covered with sandy soil, which can be easily detached. In contrast, the Mekong River Basin is dominantly covered by clay soil. This may be why SSL is not sensitive to k, and k is not important for sediment yield in the Mekong River Basin.

Fig. 7 shows the simulated results of monthly SSL compared with measurements at three gauging stations from 1991–2000. The simulated results are in good agreement with observations, as summarized in Table 3. *NSE* was larger than 0.6 for the upper, middle, and lower stations in the calibration (1991–1995) and validation (1996–2000) periods, except in the case of the validation period for the upper station (Chiang Sean) (*NSE* = 0.51). The model simulation underestimated at the upper (Chiang Sean) station (Fig. 7), and this error may have been caused by the effect of the Manwan Dam on the main stream in the upper basin of the Mekong River Basin (Lu and Siew, 2006). Nevertheless, the linear correlation coefficient (r) between simulated and observed SSL was in the range of 0.80 to 0.86 for all three stations. Generally, the SSL was fairly well simulated at the three stations (Fig. 7). The simulated results describe the seasonal pattern of SSL in the Mekong River Basin, and higher SSL is expected during the rainy season, as described also by Walling (2008). The model results reveal that, for the entire period of 1991–2000, the average annual SSL values were the

highest (8.9×10^7 t yr^{-1}) at the middle region, whereas the upper and lower regions showed average annual SSL values of 3.4×10^7 and 5.6×10^7 t yr^{-1}, respectively. Walling (2009) reported that the annual SSL is high in the middle region before increasing further downstream. Our simulated results also showed higher SSL in the middle region (i.e., Khong Chiam station) than in other regions. This is probably due to the large tributary drainage area. The annual SSL at Lower Mekong (after the Chinese boundary, including the middle region) tends to increase as basin area increases.

The simulated total annual SSL at Phnom Penh fluctuated over the period 1991–2000 (average = 6.86×10^7 t yr^{-1}). This study shows a 57% lower SSL than the reported average annual SSL (16.0×10^7 t yr^{-1}) (FAO/AGL, 2005). Lu and Siew (2006) reported the average annual SSL for the period 1962–2003 in the Mekong River Basin was about 14.5×10^7 t yr^{-1} based on rating curve estimation. The difference in SSL between those reports and our estimate here is probably due to the different locations of the control stations. In FAO/AGL (2005), SSL was estimated for the whole Mekong River Basin area, including the Mekong delta. This study covered only the area to Phnom Penh. In addition, different methods for SSL estimation could explain the variances.

The monthly SSC simulation at the stream gauging stations for the period 1991–2000 is shown in Fig. 8. The correlation coefficient *r* was larger than 0.5 between monthly observed and simulated SSC at the three gauging stations (Table 3). The overall average RMSE between the observed and simulated SSC was 0.31 at Chiang Sean, 0.25 at Khong Chiam and 0.14 kg m^{-3} at Phnom Penh. The results reveal a decreasing trend in the SSC along the three regions from upstream to the downstream (Fig. 8). The average monthly SSC was the highest at Chiang Sean station (estimated to be 0.33 kg m^{-3}). The average SSC was lowest at Phnom Penh (estimated to be 0.13 kg m^{-3}). The low value at Phnom Penh was due to the sediment deposition in the lower region. This trend was due to the decrease in the main stream water

velocity, which promotes sediment deposition and decreases SSC. In fact, a decreasing trend in mean monthly SSC was observed along the entire length of the Mekong River since water quality measurement began in 1985 (Lu and Siew, 2006). The model results also show that the SSC was higher in the rainy season (July, August, and September) than the dry season at all three stations (Fig. 8). This is due to the intensive soil erosion mainly caused by heavy precipitation in the rainy season. The high simulated SSC in July at the upper station showed a good agreement with the observed SSC, which recorded the highest concentrations occurring early in rainy season, in mid-July. After mid-August, the observed SSC began to decline, continuing to decline through early September. This trend matches the simulated SSC trend, which showed a decline in August and September.

3.2.3. Sensitivity of SSL to sediment-related parameters

A sensitivity analysis was applied for SSL in the Mekong River Basin in the same manner as in the Chao Phraya River Basin. First, all the parameters were set to calibrated values, which were k = 7 g J^{-1}, $K_{f\,=}$ 1 mg m^{-2} s^{-1}, and J = 3 kPa. The same factor was used in the Mekong River Basin and Chao Phraya River Basin in order to compare the sensitivity of the parameters for SSL in the both basins. The SSL was simulated at Khong Chiam station for all the parameters in 1999.

The results revealed that SSL increases slightly in September when k decreases by 50% from the initial (Fig. 9a). In addition, the peak SSL kept increasing and showed smaller changes with further decreases (at a factor of 25%) from the initial value. Thus, in the Mekong River Basin, SSL is less sensitive to k than in the Chao Phraya River Basin. The subtle response of SSL for different k implies that soil strength and clay content are not important, although studies of soil strength for the different group soils of sands, loams, and clays (Sharma, 1999) show that k decreases as soil strength increases. Such results from a

sensitivity analysis suggest that soil detachment by raindrop contributes little to SSL generation in the Mekong River Basin.

Regarding K_f, the peaks in SSL in 1999 decreased by 40% with the multiplying a factor of 100% (Fig. 9b) due to the increase of soil detachability from sheet flow. The simulated SSL also drastically decreased with decreasing K_f (with factors 0.1 and 0.01). The simulated SSL reveals the opposite trends from that reported by Bhattarai and Dutta (2005), who found the simulated SSL peaks from August to October increased with increasing K_f values (0.4 to 0.6 mg m^{-2} s^{-1}). This result implys that soil detached from sheet flow is important input for SSL transport in the river in the Mekong River Basin. The literature does not contain conclusive results on the sensitivity range of K_f (Lukey et al., 2000; Bathurst et al., 2002). For example, sediment modeling using K_f with a small range from 0.0019 to 0.0045 mg m^{-2} s^{-1} in New Zealand (Russell and Sandy, 2006) showed the inverse trend of the result shown in Mekong for the same range, where the simulated SSL increased with increasing K_f.

The analysis of soil cohesion (J) shows that the SSL peak in September increases by 150% with a factor of 1.25 for J (Fig. 9c). In contrast, the SSL peak decreases by 70% and 80% by decreasing the soil cohesion factor by 0.75 and 0.5, respectively. The change in SSL is more sensitive to soil cohesion than k and K_f, as soil cohesion indicates soil detachability within rivers. In the equations for net soil detachment in rivers (Eqs. 9 and 10), soil cohesion limits the detachment of sediment. Soil cohesion is recognized to be related to erodibility, and no unique relationship exists even for a single size of soil (Govers et al., 1990).

The three input parameters that describe soil erodibility have a significant influence on the output of SSL. Generally, soil cohesion (J) is the most sensitive parameter in both river basins. The SSL change was sensitive to soil detachability over land (K_f) in the Mekong, whereas SSL change was more sensitive to detachability by raindrop (k) in the Chao Phraya.

4 Conclusion

In this study, a physically-based model of sediment transport targeting a large basin scale was developed and coupled with a distributed hydrological model. The model enables us to simulate rainfall–runoff processes and sediment transport on hillslope and within a river network. In its application to the Chao Phraya River and Mekong River basins, the sediment dynamics (i.e., yield and erosion) were reasonably simulated in hillslope areas. As it is a grid-based model, it can identify locations of serious sediment dynamics by a fine grid scale. Moreover, the present model applications estimated soil cohesion (*J)* and detachability (k, K_f) in the Chao Phraya and Mekong rivers, and revealed the high sensitivity of SSL to soil detachability (k, K_f) in both basins.

However, the present model assumed a single SS size instead of a wide range of SS sizes, due to limited information in both case studies. Thus, insufficient modeling of SS size distribution might have limited the applicability of the sediment model in the case studies. Therefore, the model performance may be further improved by incorporating multi-size sediment particles into the model. Uncertainties in terms of model inputs, parameters and structure may also have influenced the simulation results. For example, the estimation of net sediment detachment (Eq. 9) could be improved by revising the equations. Currently, this equation (Eq. 9) assumed that the soil particles were detached (limitation to deposition) and limited by factors such as soil cohesion. Thus, this equation should be improved by considering the reasonable balance between erosion and deposition, especially for river basins. Sediment management in river basins is highly affected by both processes.

Nevertheless, the outputs from this model at the basin scale may provide useful information to developers, decision makers, and other stakeholders when planning and implementing appropriate basin-wide sediment management strategies, which can also be integrated with water resource management. The model could also be used also to project the anthropogenic impacts on sediment dynamics under different scenarios in large river basins.

Author contributions. S. Zuliziana and K. Tanuma made substantial contributions to model develop, simulations, data collection and analysis, and drafting and editing the manuscript. C. Yoshimura and O. C. Saavedra developed the research framework and models and helped edit the manuscript.

Acknowledgements. This research for Chao Phraya River was supported by Asian Core Program of Japan Society for the Promotion of Science (JSPS). Also, the part of the modeling work for Mekong River was supported by JSPS Core-to-Core Program (B. Asia-Africa Science Platforms) and Collaborative Research Program (CRA) of AUN/SEED-Net.

References

Ahlgren, J. and Hessel, K.: The suspended matter of Mekong. A study of the chemical constituents adsorbed to suspended matter of the Mekong River, Lao PDR. Working Paper 306, Swedish University of Agricultural Sciences, International Rural Development Centre, 1996.

Arnold, J. G., Srinivasan, R., Muttiah, R. S., and Williams, J. R.: Large area hydrologic modeling and assessment, Part I: model development, J. Am. Water Resour. As., 34, 73–89, 1998.

Bathurst, J.C., Sheffield, J., Vicente, C., White, S.M., and Romano, N.: Modelling large basin hydrology and sediment yield with sparse data: the agri basin, southern Italy, In Mediterranean Desertification: A Mosaic of Processes and Responses, Geeson NA, Brandt CJ, Thornes JB (eds), Wiley: Chichester, 397–415, 2002.

Bhattarai, R. and Dutta, D.: Analysis of soil erosion and sediment yield using empirical and process based models, Proceedings of the MTERM International Conference, AIT, 215–226, 2005.

Brandt, C. J.: The size distribution of throughfall drops under vegetation canopies, Catena, 16, 507–524, 1989.

Brandt, C. J.: Simulation of size distribution and erosivity of raindrops and throughfall drops, Earth Surf. Proc. Land., 15, 687–689, 1990.

Brune, G. M.: Trap efficiency of reservoirs. Trans. AGU, 34, 407–418, 1953.

Duan, Q., Soorooshian, S., and Gupta, V.: Effective and efficient global optimization for conceptual rainfall-runoff models, Water Resour. Res., 28, 1015–1031, 1992.

Duna, S., Wua, J. Q., Elliot, W. J., Robichaudb, P. R., Flanaganc, D. C., Frankenbergerc, J. R., Brownb, R. E., and Xud, A. C.: Adapting the Water Erosion Prediction Project (WEPP) model for forest applications, J. Hydrol., 366, 46–54, 2009.

FAO/AGL: World river sediment yields database, FAO, Rome, 2005.

FAO: The digital soil map of the world and derived soil properties, version 3.6, FAO/UNESCO: Rome, Italy, 2003.

Fu K.D., He D.M., and Li S.J.: Response of downstream sediment to water resource development in mainstream of the Lancang River, Chinese Sci. Bull., 51, 119–126, 2006.

Govers, G.: Empirical relationships for the transport capacity of overland flow, in erosion, transport and deposition processes, IAHS Publ., 189, 45–63, 1990.

Gumiere, S. J., Le Bissonnais, Y., and Raclot, D.: Soil resistance to interill erosion: model parameterization and sensitivity, Catena, 77, 274–284, 2009.

Habib-ur-Rehman, M. and Naeem Akhtar, M.: Development of regional scale soil erosion and sediment transport model; its calibration and validations, Pakistan Engineering Congress, 69th Annual Session Proceedings, 2004.

Kabir, M. A., Dutta, D., and Hironaka, S.: Process-based distributed modeling approach for analysis of sediment dynamics in a river basin, Hydrol. Earth Syst. Sci., 15, 1307–1321, 2011.

Kite, G.: Modelling the Mekong: hydrological simulation for environmental impact studies, J. Hydrol., 253, 1–13, 2001.

Kummu, M., Lu, X. X., and Varis, O.: Basin-wide trapping efficiency of emerging reservoirs long the Mekong, Geomorphology, 119, 181–197, 2010.

Kyuma, K.: Paddy soils in the Mekong Delta of Vietnam. Discussion paper 85, Center for Southeast Asian Studies, Kyoto University, Kyoto, 77p, 1976.

Lu, X. X. and Siew, R. Y.: Water Discharge and sediment flux changes over the past decades in the Lower Mekong River: possible impact of the Chinese dams, Hydrol. Earth Syst. Sci., 10, 181–195, 2006.

Lukey, B.T., Sheffield, J., Bathurst, J.C., Hiley, R.A., and Mathys, N.: Test of the SHETRAN technology for modeling the impact of reforestation on badlands runoff and sediment yield at Draix, France, J. Hydrol., 235, 44–62, 2000.

MRC: Lower Mekong Hydrologic Yearbook, Mekong River Comm., 2000.

MRC: Annual report 2005 [CD-ROM], Vientiane, Mekong: Mekong River Comm., 2005.

Milliman, J.D. and Meade, R.H.: World-wide delivery of river sediment to the oceans, J. Geol., 91, 1–21, 1983.

Morgan, R. P. C., Quinton, J. N., Smith, R. E., Govers, G., Poesen, W. A., Auerswald, K., Chisci, G., Torri, D., and Styczen, M. E.: The European Soil Erosion Model (EU-ROSEM): A dynamic approach for predicting sediment transport from fields and small catchments, Earth Surf. Proc. Land., 23, 527–544, 1998.

Morgan, R. P. C.: A simple approach to soil loss prediction: a revised Morgan-Morgan-Finney model, Catena, 44, 305–322, 2001.

Nash, J.E. and Sutcliffe, J.V.: River flow forecasting through, Part I, a conceptual models discussion of principles, J. Hydrol., 10, 282–290, 1970.

Nearing, M. A., Jetten, V., Baffaut, C., Cerdan, O., Couturier, A., Hernandez, M., Bissonnais, L. Y., Nichols, M. H., Nunes, J. P., Renschler, C. S., Souchere, V., and Oost K. V.: Modeling response of soil erosion and runoff to changes in precipitation and cover, Catena, 61, 131–154, 2005.

Neitsch, S. L.: Soil and water assessment tool user's manual version 2000, SWRL report 202, 02–06, 2002.

Ongley, E.: Sediment Measurement, Chap. 13, In: Water Quality Monitoring, (Ed.), Design And Implementation Of Fresh Water Quality Studies And Monitoring Programmes,

World Health Organization, Geneva, 1996.

Ponce, V. M.: Engineering hydrology: principles and practices, Vol. 640, Englewood Cliffs, Prentice Hall, 1989.

Rauws, G. and Govers, G.: Hydraulic and soil mechanical aspects of rill generation on agricultural soils, J. Soil Sci., 39, 111–124, 1988.

Renard, K. G. and Freimund, J. R.: Using monthly precipitation data to estimate the R-factor in the revised USLE, J. Hydrol., 157, 287–306, 1994.

Roberto, R., Thanh, H., and Maria, C.: A RUSLE approach to model suspended sediment load in the Lo river (Vietnam): effects of reservoirs and land use changes, J. Hydrol., 422–423, 17–29, 2012.

Russell, A. and Sandy, E.: Physically based modeling of sediment generation and transport under a large rainfall simulator, Hydrol. Process, 20, 2253–2270, 2006.

Santhi, C., Arnold, J. G., Williams, J. R., Dugas, W. A., Srinivasan, R., and Hauck, L. M.: Validation of the SWAT model on a large river basin with point and nonpoint sources, J. Am. Water Resour. As., 37, 1169–1188, 2001.

Sharma, P. P., Gupta, S. C., and Foster, G.R.: Raindrop-induced soil detachment and sediment transport from interill areas, Soil Sci. Soc. Am. J., 59, 727-734, 1995.

Tacio, H. D.: Sloping Agricultural Land Technology (SALT): a sustainable agroforestary scheme for uplands. Agroforest Syst., 22, 145–152, 1993.

Thai Meteorological Department: Weather outlook for Thailand during rainy season (June–October 2012), Bangkok, Thailand: Thai Meteorological Department, 2012.

Torri, D., Sfalanga, M., and Delsette, M.: Splash detachment–runoff depth and soil cohesion, Catena, 14, 149–155, 1987.

UNEP Environment Asessment Programe for Asia and the Pacific Bangkok: Land cover assessment and monitoring, Environment assessment technical reports, Volume 8-A, 1997.

Valeriano, O. C. S., Koike, T., Yang, K., and Yang, D.: Optimal dam operation during flood season using a distributed hydrological model and a heuristic algorithm, J. Hydrol. Eng., 15, 580–586, 2010.

Walling, D. E. and Fang, D.: Recent trends in the suspended sediment loads of the world's rivers, Global Planet. Change, 39, 111–126, 2003.

Walling, D. E.: Evaluation and analysis of sediment data from the Lower Mekong River, Report to the Mekong River Commission, 61, 2005.

Walling, D. E.: The Changing Sediment Load of the Mekong River, Ambio, 37, 150–157, 2008.

Walling, D. E.: The sediment load of the Mekong River, In Campbell I. C. (Ed), The Mekong Biophysical environment of an international river basin, Elsevier, New York, 113–142, 2009.

Walling, D.E.: Human Impact on the sediment load of Asian rivers, sediment problems and sediment management in Asian rivers basin, IAHS Publ., 349, Walling ford, 37–51, 2011.

Wang, J. J., Lu, X. X., and Kummu, M.: Sediment load estimates and variations in the Lower Mekong River, River Res. Appl., 27, 33–46, 2011.

Wischmeier, W.H. and Smith, D.D.: Predicting rainfall erosion soil losses: a guide to conservation planning, Agriculture Handbook, No. 282, No. 537, US Department of Agriculture Research Service, 244–252, 1978.

Yang, D., Herath, S., Oki, T., and Musiake, K.: Application of distributed hydrological model in the Asian monsoon tropic region with a perspective of coupling with atmospheric models, J. Meteorol. Soc. Japan, 79, 373–385, 2001.

Yang, D., Kanae, S., Oki, T., Koike, T., and Musiake, K.: Global potential soil erosion with reference to land use and climate changes, Hydrol. Process., 17, 2913–2928, 2003.

Zarfl, C., Lumsdon, A.E., Berlekamp, J., Tydecks, L., and Tockner, K.: A global boom in hydropower dam construction, Aquat. Sci., doi: 10.1007/s00027-014-0377-0, 2014.

Table 1. Model parameters calibrated for Chao Phraya River and Mekong River basins.

	Chao Phraya River	Mekong River
Hydrological model		
Saturated hydraulic conductivity of surface soil, *ksat1* (mm hr^{-1})	89.0 – 255.6	4.6 – 30.4
Residual soil moisture, *wrsd* (mm hr^{-1})	0.16 – 0.17	0.16 – 0.19
Sediment model		
Raindrop, k (g J^{-1})	7.0 – 9.1	7.0 – 100.0
Overland flow, K_f (mg m^{-2} s^{-1})	0.6 – 1.1	1.0 – 10.0
Soil cohesion, J (kPa)	3.0 – 7.5	3.0 – 5.0

Table 2. Model performance indicators for monthly river discharge, SSL, and SSC in Chao Phraya River Basin from 2001 to 2010. *NSE* and *r* stands for the Nash-Sutcliffe Efficiency coefficient and correlation coefficient, respectively.

Stations		Performance Indicators			
Location	Code	Calibration (2001)		Validation (2002-2010)	
		NSE	*r*	*NSE*	*r*
River discharge					
Ping River	P73	0.88	0.94	0.89	0.95
Wang River	W3A	0.90	0.89	0.91	0.90
Yom River	Y37	0.81	0.95	0.82	0.96
Nan River	N13A	0.82	0.93	0.83	0.94
Chao Phraya River	C2	0.68	0.93	0.69	0.94
Suspended sediment load (SSL)					
Ping River	P73	0.54	0.70	0.55	0.71
Wang River	W3A	0.76	0.43	0.78	0.45
Yom River	Y37	0.49	0.50	0.51	0.51
Nan River	N13A	0.70	0.80	0.72	0.80
Chao Phraya River	C2	-0.14	0.29	-0.15	0.31
Suspended sediment concentration (SSC)					
Ping River	P73	-1.96	0.15	-1.21	0.52
Wang River	W3A	-0.11	0.57	-0.27	0.61
Yom River	Y37	No observation		0.28	0.57
Nan River	N13A	-0.05	0.68	-1.94	0.62
Chao Phraya River	C2	0.52	0.45	-3.24	0.10

Table 3. Model performance indicators for monthly river discharge, SSL, and SSC in Mekong River Basin from 1991 to 2000. *NSE* and *r* stands for the Nash-Sutcliffe Efficiency coefficient and correlation coefficient, respectively.

Stations		Performance Indicators			
Location	Code	Calibration (1991-1995)		Validation (1996-2000)	
		NSE	*r*	*NSE*	*r*
River discharge					
Chiang Sean	1	0.71	0.81	0.71	0.86
Khong Chiam	2	0.77	0.87	0.74	0.86
Phnom Penh	3	0.84	0.87	0.85	0.86
Suspended sediment load (SSL)					
Chiang Sean	1	0.62	0.85	0.51	0.65
Khong Chiam	2	0.62	0.86	0.62	0.83
Phnom Penh	3	0.64	0.80	0.64	0.87
Suspended sediment concentration (SSC)					
Chiang Sean	1	0.08	0.58	-4.33	0.31
Khong Chiam	2	-0.07	0.43	-0.25	0.73
Phnom Penh	3	-0.07	0.66	-1.02	0.78

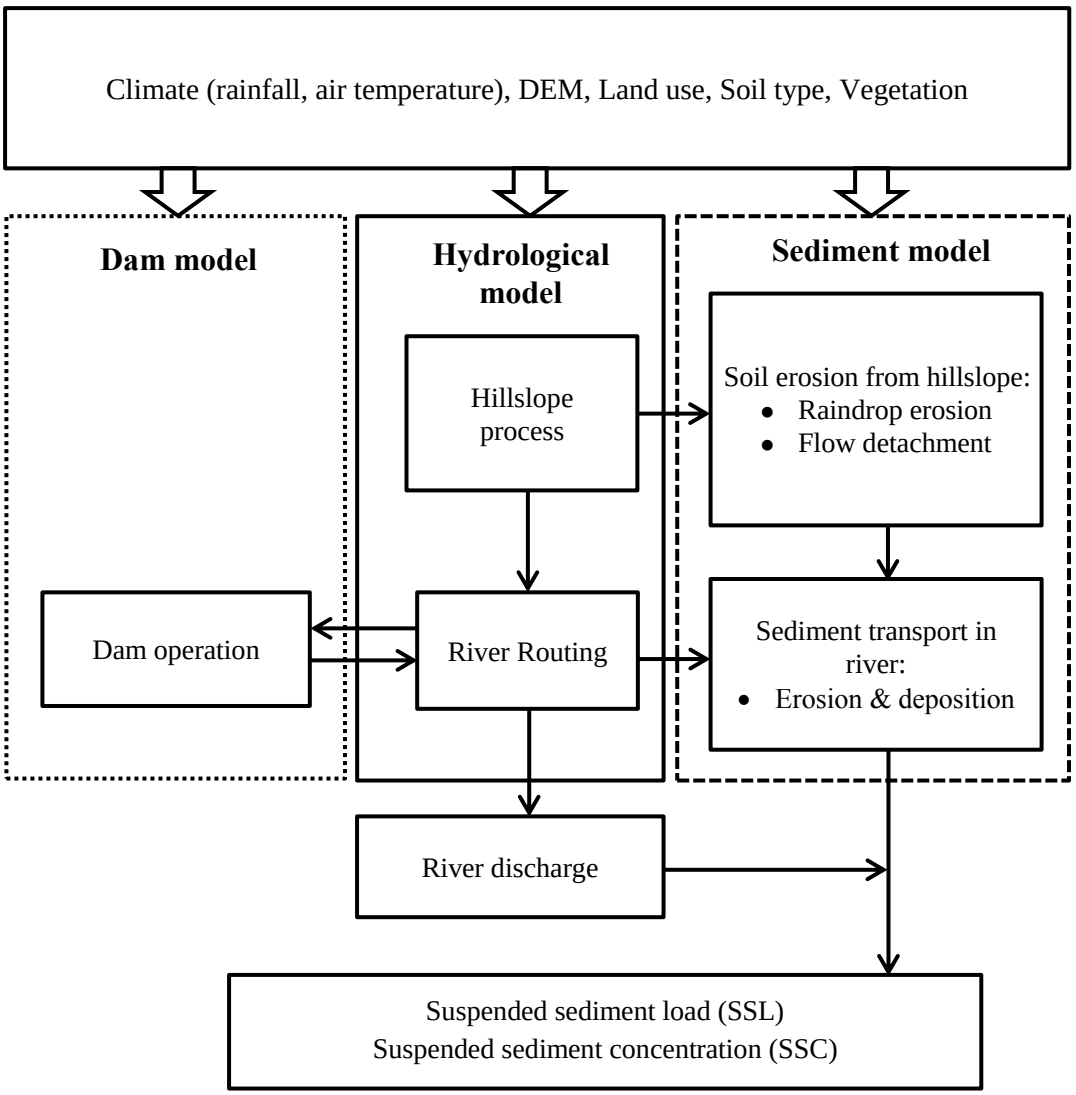

Figure 1. Structure of the distributed sediment model integrated with a process-based distributed hydrological model.

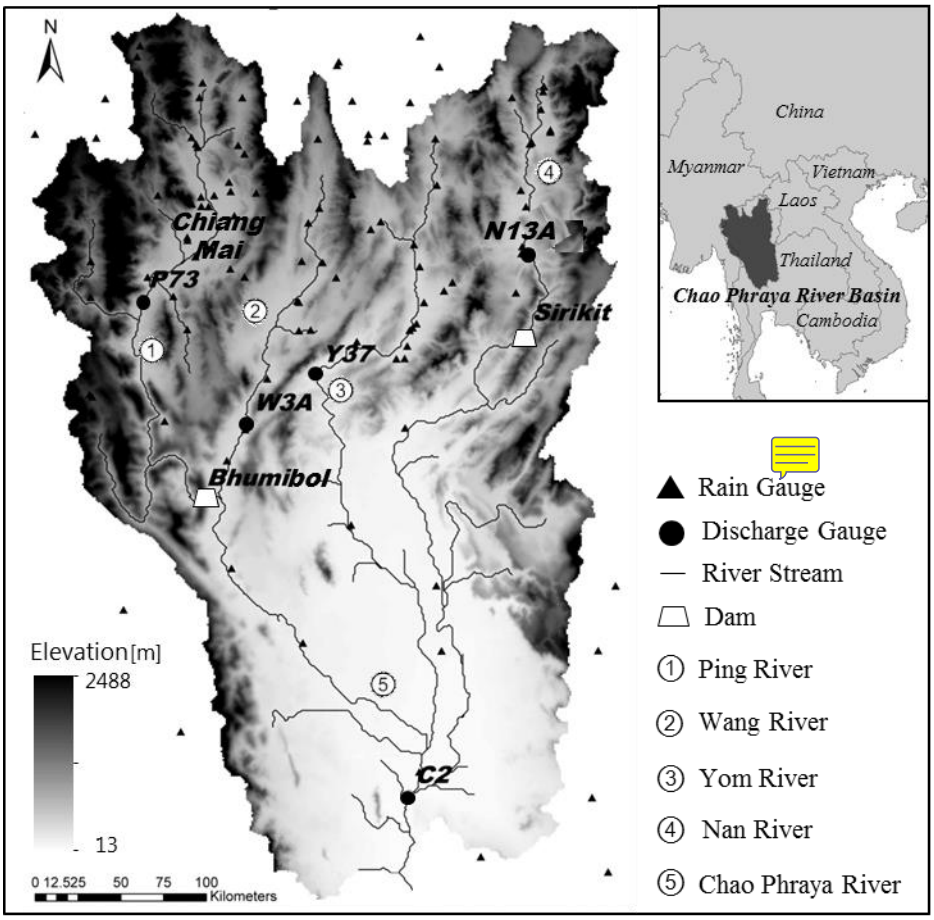

Figure 2. The target area of Chao Phraya River Basin.

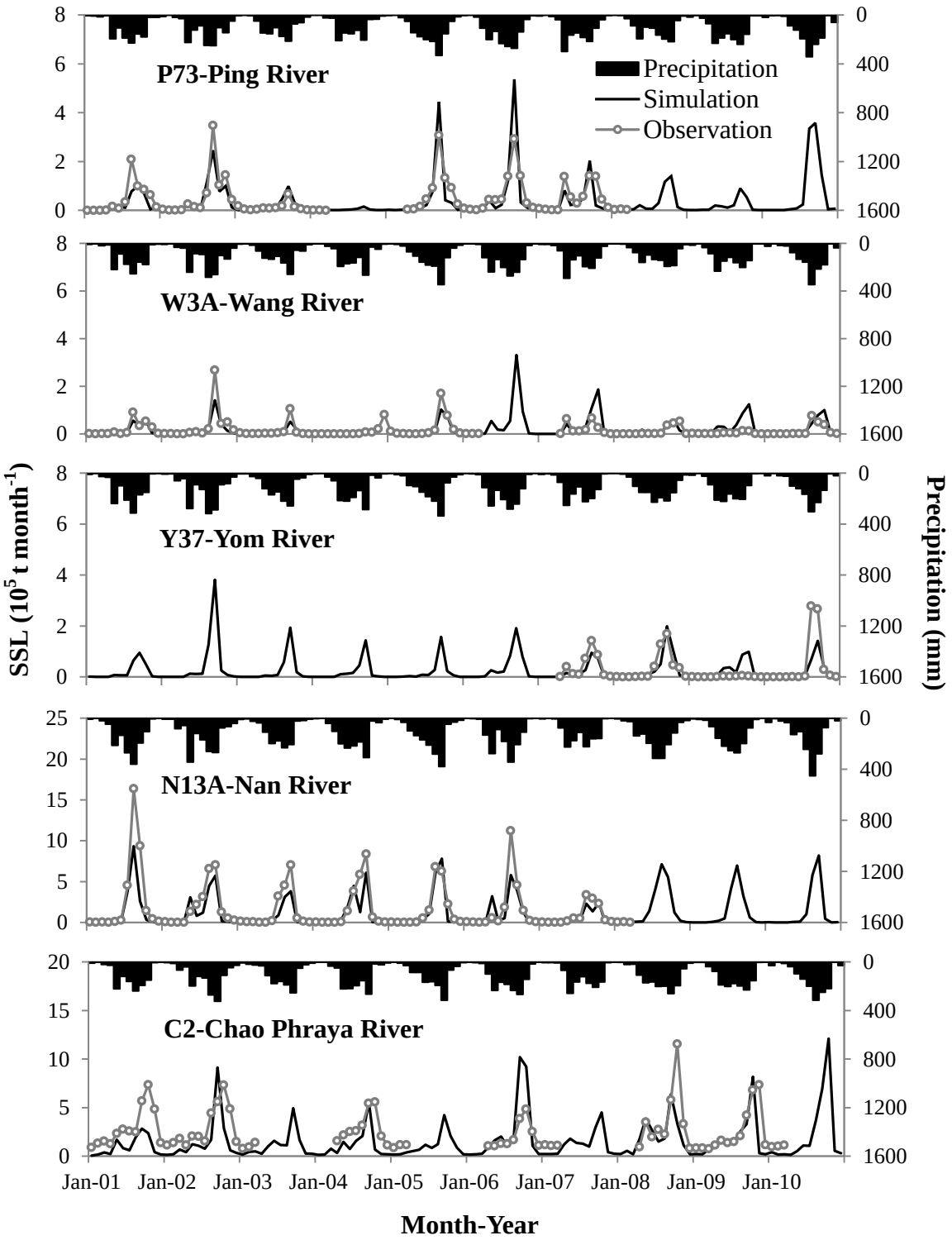

Figure 3. Monthly suspended sediment load (SSL) at stream gauge stations in Chao Phraya River Basin for 2001-2010.

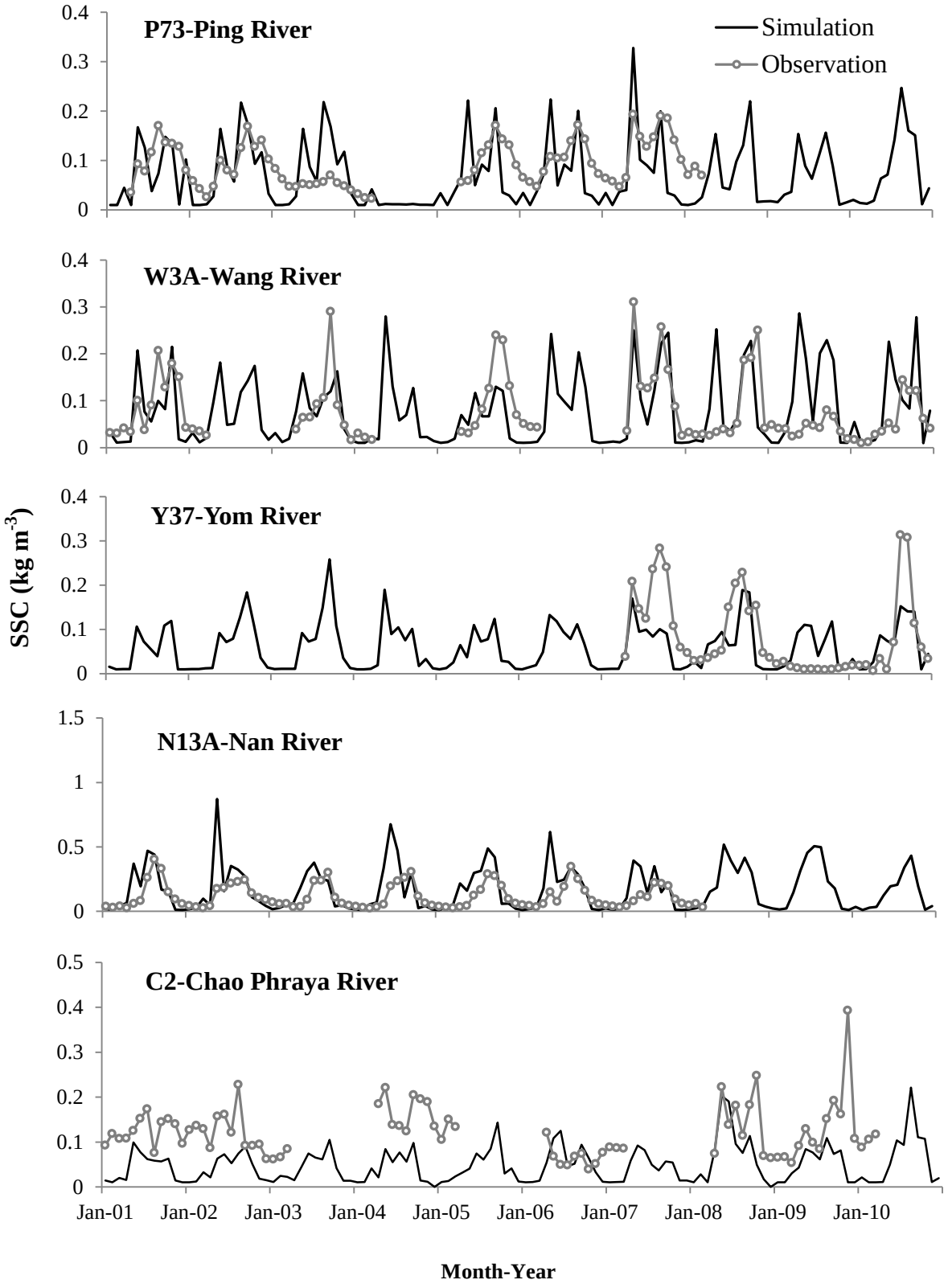

Figure 4. Average monthly suspended sediment concentration (SSC) at stream gauge stations in Chao Phraya River Basin for 2001-2010.

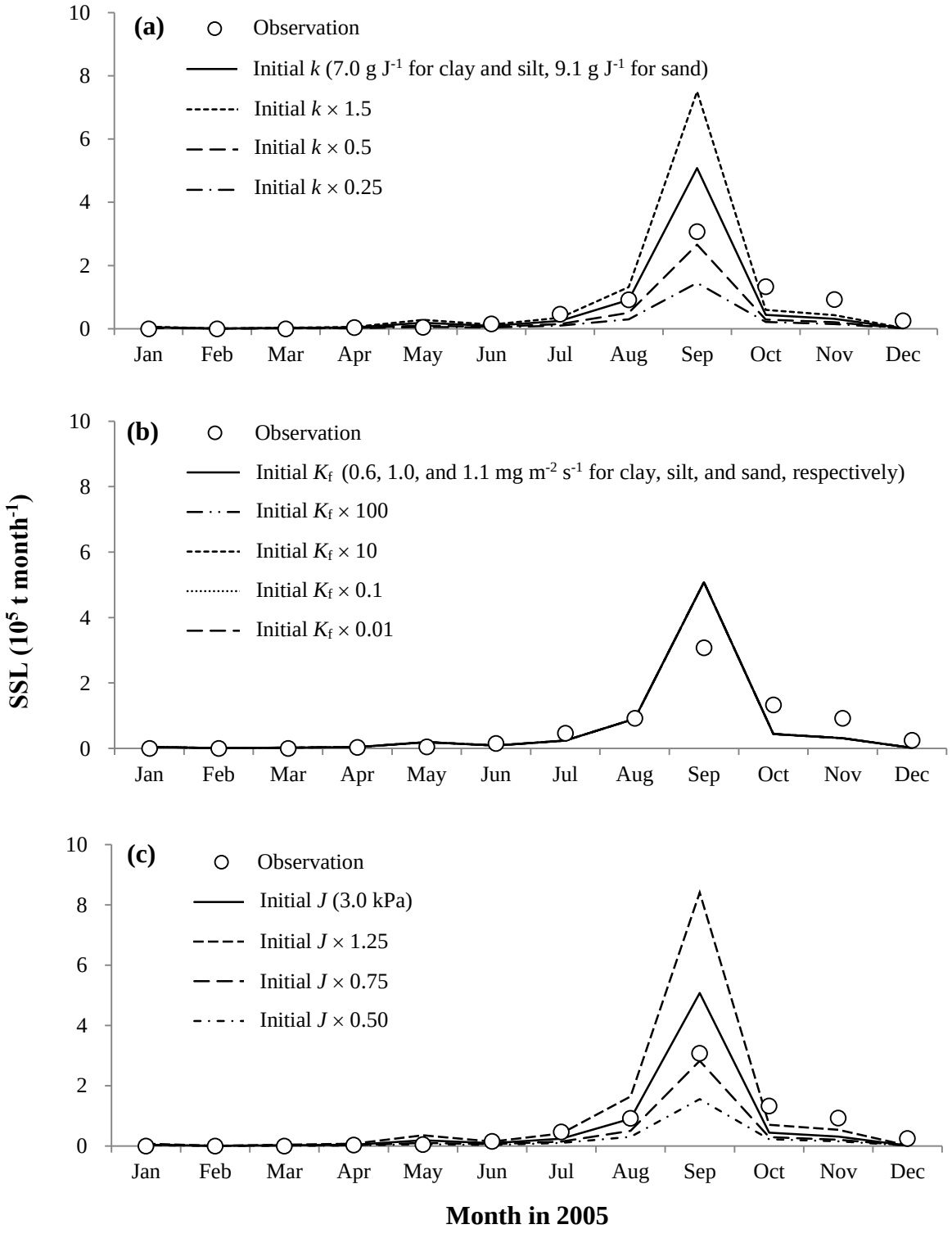

Figure 5. Sensitivity of suspended sediment load (SSL) at P73 in Chao Phraya River Basin to **(a)** detachability from rain drop (k), **(b)** detachability from sheet flow (K_f) and **(c)** soil cohesion (J). Difference among lines in Figure **(b)** is invisible due to the minor response of SSL to K_f.

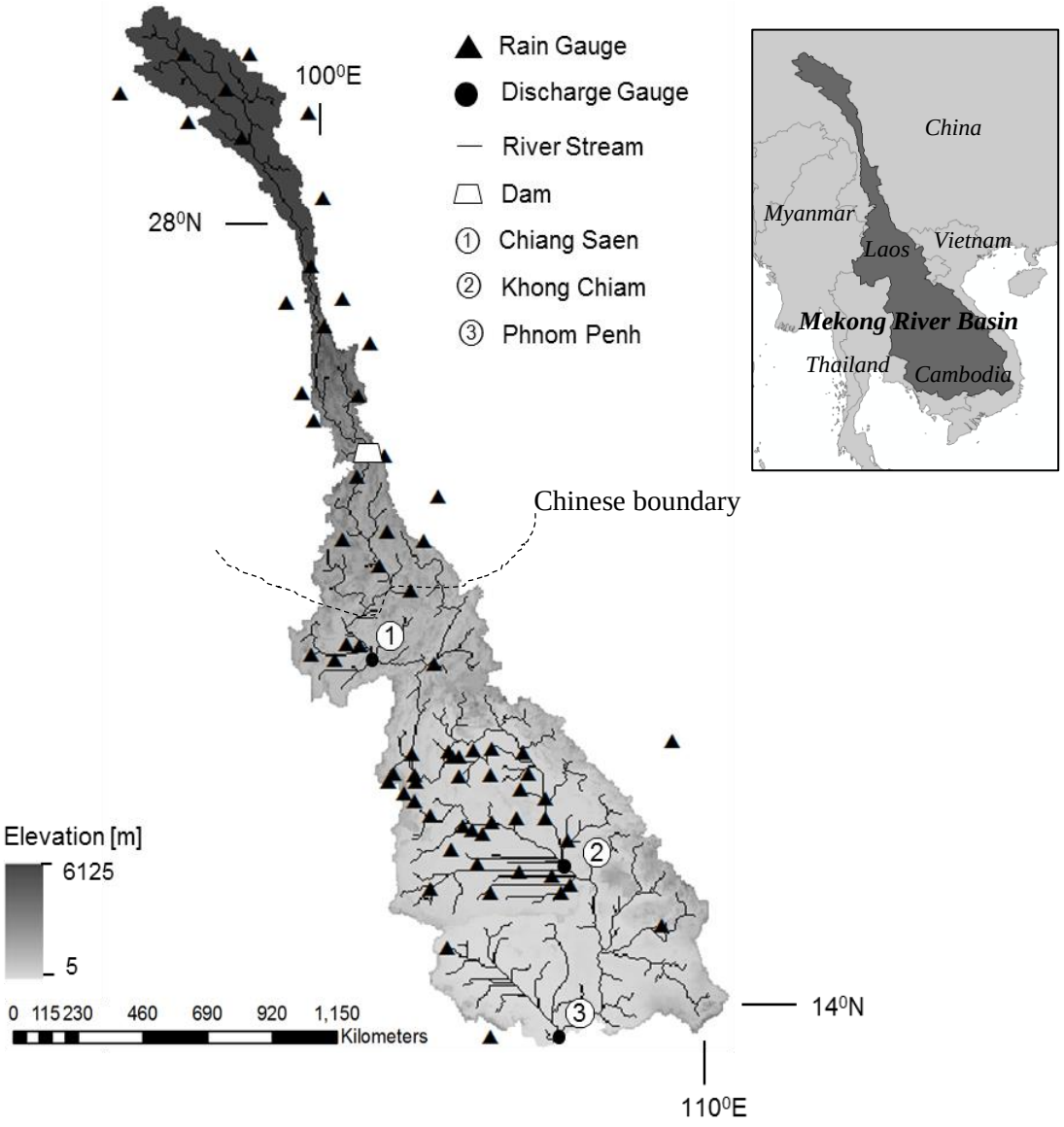

Figure 6. The target area and the modelled river network of Mekong River Basin.

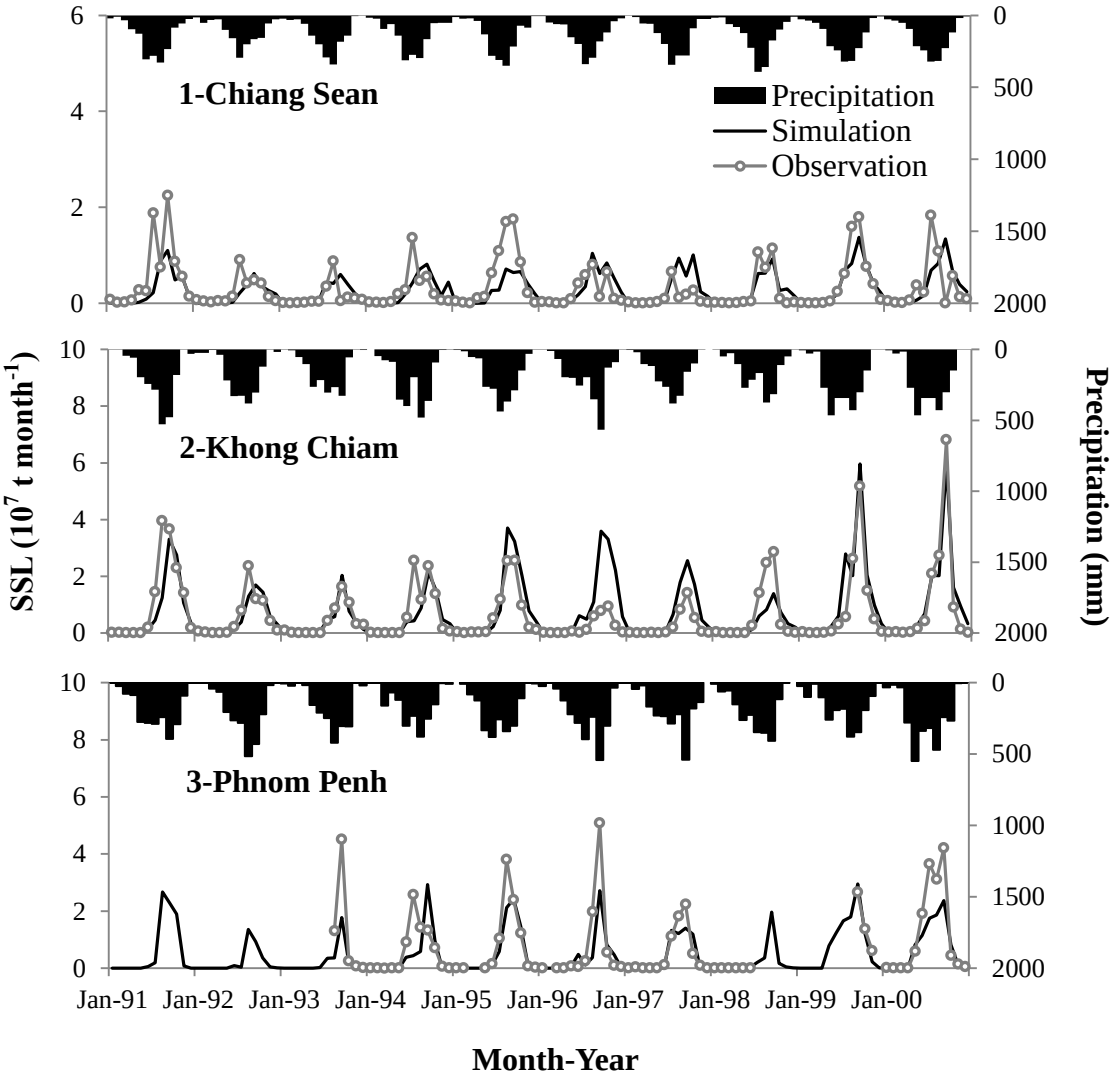

Figure 7. Monthly suspended sediment load (SSL) at stream gauge stations in the Mekong River Basin for 1991 – 2000.

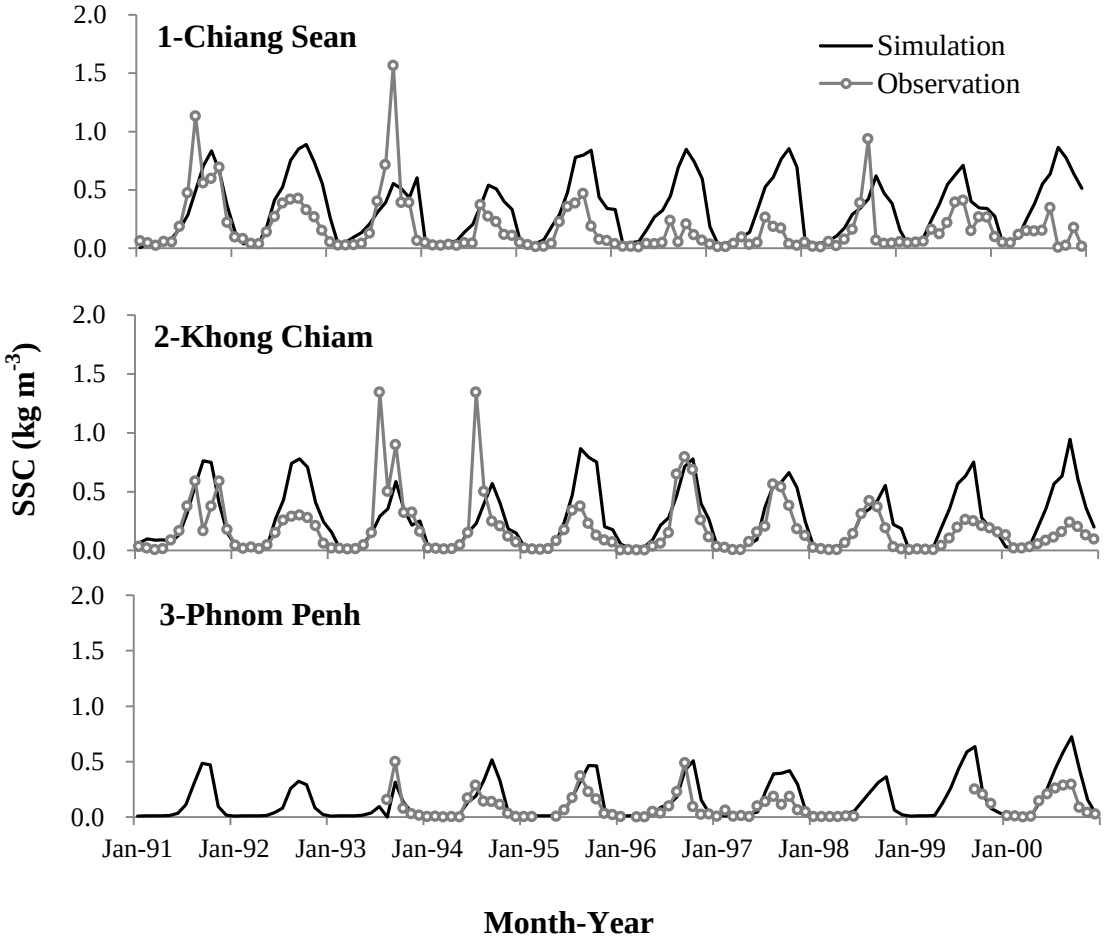

Figure 8. Monthly suspended sediment concentration (SSC) at stream gauge stations in Mekong River Basin for 1991-2000.

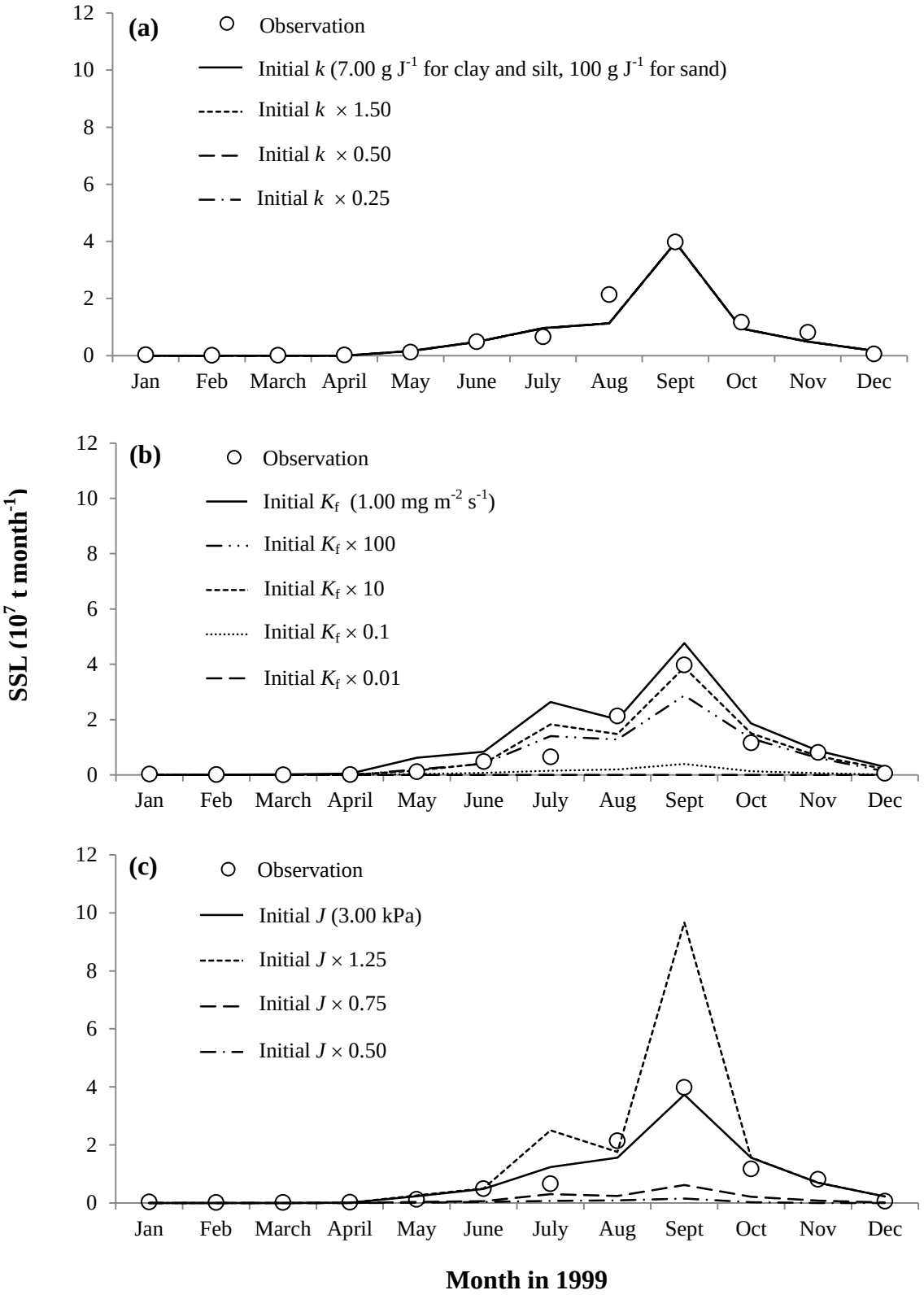

Figure 9. Sensitivity of suspended sediment load (SSL) at Khong Chiam station in Mekong River Basin to **(a)** detachability from rain drop (k), **(b)** detachability from sheet flow (K_f), **(c)** soil cohesion (J). Difference among lines in Figure **(a)** is invisible due to the minor response of SSL to k.

Appendix A

Monthly average river discharge at stream gauge stations from 2001 to 2010 at Chao Phraya River Basin.

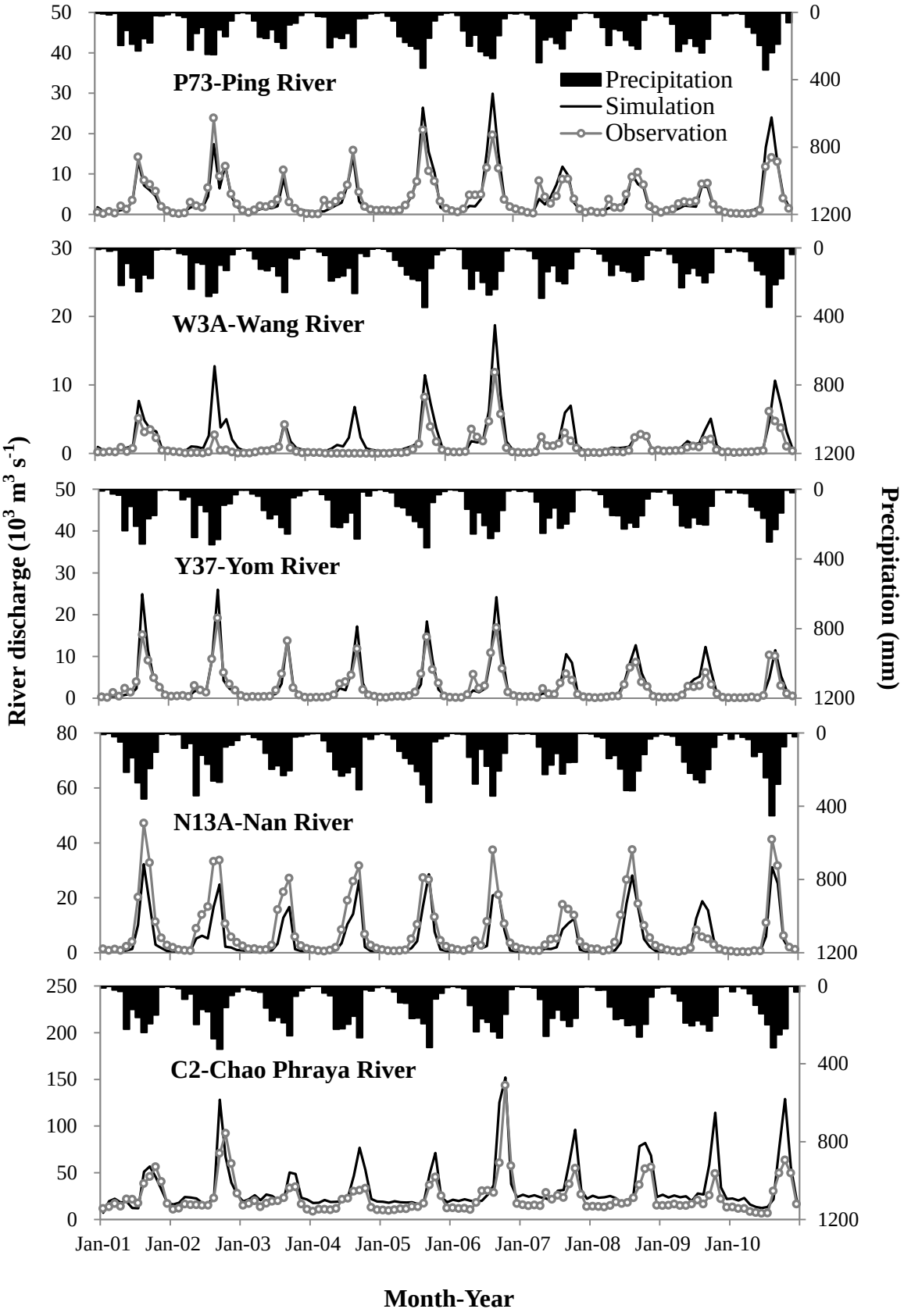

Appendix B

Monthly average river discharge at stream gauge stations from 1991 to 2000 at Mekong River Basin.